PROCEEDINGS B

royalsocietypublishing.org/journal/rspb

Research

Cite this article: Nesher N, Maiole F, Shomrat T, Hochner B, Zullo L. 2019 From synaptic input to muscle contraction: arm muscle cells of *Octopus vulgaris* show unique neuromuscular junction and excitation–contraction coupling properties. *Proc. R. Soc. B* **286**: 20191278.
http://dx.doi.org/10.1098/rspb.2019.1278

Received: 5 June 2019
Accepted: 4 August 2019

Subject Category:
Development and physiology

Subject Areas:
neuroscience, physiology

Keywords:
cephalopods, neuromuscular junction, CICR, ACh receptors, E-C coupling, dihydropyridine and ryanodine

Authors for correspondence:
Nir Nesher
e-mail: nir.nesher@mail.huji.ac.il
Letizia Zullo
e-mail: letizia.zullo@iit.it

Electronic supplementary material is available online at https://dx.doi.org/10.6084/m9.figshare.c.4614131.

THE ROYAL SOCIETY PUBLISHING

From synaptic input to muscle contraction: arm muscle cells of *Octopus vulgaris* show unique neuromuscular junction and excitation–contraction coupling properties

Nir Nesher[1], Federica Maiole[2,3], Tal Shomrat[1], Benyamin Hochner[4] and Letizia Zullo[2,5]

[1]Faculty of Marine Sciences, Ruppin Academic Center, Michmoret, Israel
[2]Center for Synaptic Neuroscience and Technology, Istituto Italiano di Tecnologia, Largo Rosanna Benzi 10, 16132 Genova, Italy
[3]Department of Experimental Medicine, University of Genova, Viale Benedetto XV, 3, 16132 Genova, Italy
[4]Department of Neurobiology, Alexander Silberman Institute of Life Sciences, Hebrew University of Jerusalem, Jerusalem, Israel
[5]IRCSS, Ospedale Policlinico San Martino, Largo Rosanna Benzi 10, 16132 Genova, Italy

LZ, 0000-0003-0503-6312

The muscular-hydrostat configuration of octopus arms allows high manoeuvrability together with the efficient motor performance necessary for its multitasking abilities. To control this flexible and hyper-redundant system the octopus has evolved unique strategies at the various levels of its brain-to-body organization. We focus here on the arm neuromuscular junction (NMJ) and excitation–contraction (E-C) properties of the arm muscle cells. We show that muscle cells are cholinergically innervated at single eye-shaped locations where acetylcholine receptors (AChR) are concentrated, resembling the vertebrate neuromuscular endplates. Na^+ and K^+ contribute nearly equally to the ACh-activated synaptic current mediating membrane depolarization, thereby activating voltage-dependent L-type Ca^{2+} channels. We show that cell contraction can be mediated directly by the inward Ca^{2+} current and also indirectly by calcium-induced calcium release (CICR) from internal stores. Indeed, caffeine-induced cell contraction and immunohistochemical staining revealed the presence and close association of dihydropyridine (DHPR) and ryanodine (RyR) receptor complexes, which probably mediate the CICR. We suggest that the dynamics of octopus arm contraction can be controlled in two ways; motoneurons with large synaptic inputs activate vigorous contraction via activation of the two routs of Ca^{2+} induced contraction, while motoneurons with lower-amplitude inputs may regulate a graded contraction through frequency-dependent summation of EPSP trains that recruit the CICR. Our results thus suggest that these motoneuronal pools are likely to be involved in the activation of different E-C coupling modes, thus enabling a dynamics of muscles activation appropriate for various tasks such as stiffening versus motion generation.

1. Introduction

The body of *Octopus vulgaris* lacks a rigid skeleton, posing two main problems for its motor control. (i) How is movement created in a structure without a rigid skeleton? And (ii) considering that the flexible arm has infinite degrees of freedom (DOFs), how is movement planned and controlled in space and time?

Octopus arms are composed mainly of muscle cells intermingled with a complex matrix of connective tissue. Together they form a flexible and incompressible organ working as a 'muscular-hydrostat' [1] (figure 1). The arm's

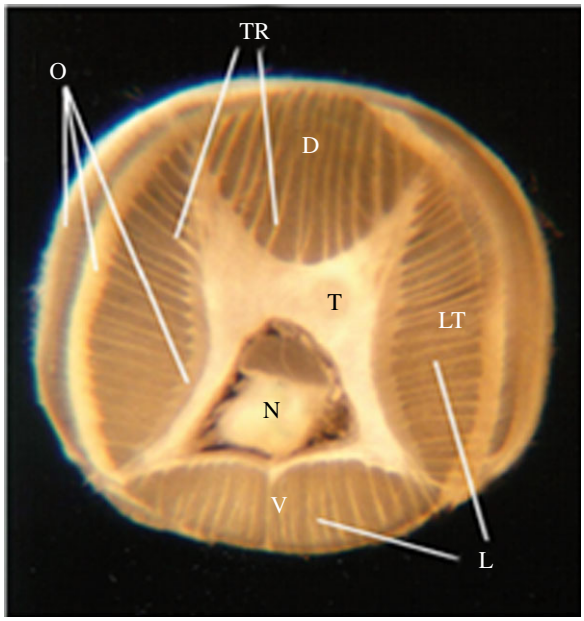

Figure 1. Transverse section of an octopus arm (modified from [2]) with the ventral (V), dorsal (D), and lateral (LT) aspects of the arm marked. The l axial nerve cord (N) runs along the longitudinal axis of each arm and is surrounded by transverse muscles (T). Oblique muscles (O) are arranged in thin external layers. Longitudinal muscles (L) are organized in four groups located at each side of the arm. The trabecula (TR) are small transverse muscle strips located within the longitudinal muscles.

intrinsic musculature is organized very compactly: thin external oblique muscle strips (O) enclose four groups of longitudinal muscles (L) running along the arm, and a central core of transverse muscles (T) encircling the arm's axial nerve cord (N). Thinly spaced muscle strips with transverse orientation (trabeculae, TR) are interlaced with each bulk of longitudinal muscles [3].

The principle of movement generation in muscular hydrostats is the 'constant volume' constraint, which provides the essential antagonistic relationship among the muscle groups organized in different orientations—the constant volume of the arm means that any contraction in one orientation affects the length of other muscle groups. Functionally, a muscular hydrostatic organization can offer both 'skeletal-like' support by stiffening, as well as forces to produce actuation that generates movement [4–8]. Muscle stiffening is the main mechanism used to create quasi-articulated structures in stereotypical arm movements like fetching, reaching and walking [9,10]. The combination of contractions of any of these muscle groups at different locations along the arm results in various arm deformations and allows the animal to produce complex movements [8]. Octopuses can, for example, grasp objects, probe surfaces, perform reaching and fetching tasks, and pass their arms and bodies through small holes, burrows, tunnels and cracks [11–13]. Controlling this soft body and flexible arms requires a highly sophisticated nervous and neuromuscular system, which in the octopus has been shown to have evolved a unique organization [14–21].

The octopus arm consists mainly of obliquely striated, long (approx. 0.9 mm) and narrow (5–10 µm) muscle cells, ending with a spindle-like shape [2]. Previous studies have shown that these cells have unique neuromuscular properties, as follows. (i) The muscle cells are electrotonically compact or iso-potential (i.e. electrical signals do not decrement along the cell). (ii) They lack Na^+ action potentials and when stimulated generate a fast calcium action potential (AP) [7,22]. (iii) Each of the arm muscle cells receives three types of discrete motoneuronal synaptic inputs; two with low quantal amplitude and slow rise times and one with an unprecedented large quantal amplitude (approx. 25 mV) and fast rise time [7,22]. (iv) No clear differences were found in these properties among cells located in different muscle groups [10].

The aim of the work here was to elucidate the structure of the neuromuscular junction (NMJ) and the excitation–contraction (E-C) coupling properties of the arm muscle cells and the role of Ca^{2+} in order to deduce the modulation of muscle cell response to synaptic inputs. This characterization is important for understanding the transformation of neural signals into motor action in this unique neuromuscular system and how this is used to achieve the highly coordinated motor actions of the flexible hyper-redundant octopus arms.

2. Methods

(a) Animal maintenance and care

Specimens of *Octopus vulgaris* were collected during spring and summer by local anglers from the Mediterranean Sea. The octopuses were housed individually in 50 × 50 × 80 cm glass aquaria containing artificial seawater prepared with synthetic marine salt (Red Sea salt). The water was continuously circulated in a closed system and filtered through coral dust and active charcoal. Aquaria were regulated to 17°C, a 12/12 h light/dark cycle, and the octopuses were fed with fish meat every other day. Animals were left to adapt to captivity for at least 10 days before use.

Particular attention was paid to housing, animal care, and health monitoring. The quality of the water was checked routinely for all relevant chemical/physical water parameters to prevent unhealthy or stressful conditions for the animals. The Guidelines for the Care and Welfare of Cephalopods in Research published by Fiorito *et al.* [23,24] were followed.

(b) Cell isolation and length measurements

Animals were anaesthetized in cold seawater containing 2% ethanol. A segment (not exceeding 1/3 of the total arm length) of one arm was amputated. The arm was cut transversely at designated locations to obtain several segments approximately 0.5 cm thick. Small pieces of arm transverse or longitudinal intrinsic musculature were dissected out (figure 1) under a dissecting microscope. The tissue was incubated at 25–30°C for 4–6 h in 0.2% collagenase (Sigma type I) dissolved in L15 culture medium (Biological Industries, Bet Ha'emek, Israel) and adjusted to the concentration of salt in seawater. The enzymatic treatment was terminated by rinsing with fresh L15. The tissue was then manually triturated until an appreciable concentration of dissociated cells could be detected in the supernatant. These cells were kept at 17°C and an aliquot of the cells was transferred to a plastic Petri dish mounted on an inverted microscope. The cells settled on the bottom of the dish within a few minutes and were subsequently video recorded using a phase-contrast optics microscope (Eclipse Ti-S Inverted Research Microscope, Nikons) and measured with ImageJ software.

(c) Electrophysiological measurements

All the electrophysiological measurements were performed with an Axoclamp 2B (Axon Instruments) amplifier in whole-cell single-patch-electrode configuration. Recordings were sampled at 20 kHz, digitally stored and analysed with LabVIEW software.

During the experiments, cells were continuously superfused with oxygenated normal artificial seawater (ASW) at room temperature. An additional system allowed the rapid application of drugs in close proximity to the cells. Glass pipettes were pulled on a pp-830 puller (Narishige) using a two-step procedure. The resistance of the pipettes was between 2 and 4 MΩ. The occurrence of contraction in the patched muscle cell was visually inspected.

(i) Current clamp

The membrane potential of isolated arm muscle cells was measured in a whole-cell current clamp in the single-patch-electrode bridge mode. After establishing the whole-cell configuration, the cell membrane potential was held at −80 to 90 mV by manually adjusting the DC current. Muscle cell responses were then induced by puffing ACh (10 mM, 5–10 nl/s) through a glass micropipette mounted on a micromanipulator. This allowed the pipette to be placed in specific positions along the cell. The puffing pressure was manually adjusted and the time and duration of the puff were set with an electronic valve.

(ii) Voltage clamp

The electrical properties of the isolated muscle cells were investigated in a whole-cell voltage-clamp in single-patch-electrode discontinuous mode. The rate of the discontinuous voltage clamp was adjusted to between 5 and 10 kHz. A discrepancy of less than or equal to 10% between the command potential and the measured potential was allowed.

(iii) Solutions and drugs

The superfusion solution (ASW) contained (in mM) 460 NaCl, 10 KCl, 55 $MgCl_2$, 11 $CaCl_2$, 10 glucose, and 10 HEPES, pH 7.6 (adjusted with NaOH) and was delivered through a peristaltic pump system allowing a replacement of the bath volume in approximately 30 s.

The patch pipettes were filled with the following internal solution (in mM): 475 K-gluconate, 2 $MgCl_2$, 1 $CaCl_2$, 5 Na_2ATP, 0.5 Na_2GTP, and 50 HEPES, buffered to pH 7.2 with KOH. The Ca^{2+}-free solutions contained (in mM): 460 NaCl, 10 KCl, 57 $MgCl_2$, 1 EGTA, 8 $CoCl_2$, 10 glucose, and 10 HEPES, pH 7.6 (adjusted with NaOH). In Ca^{2+}-free experiments the patch pipettes were filled with the following internal solution (in mM): 475 K-gluconate, 3 $MgCl_2$, 5 Na_2ATP, 0.5 Na_2GTP, and 50 HEPES, buffered to pH 7.2 with KOH. Na^+-free solution was prepared by replacing NaCl with the osmotically equivalent amount of Tris-Cl.

(d) Gene identification

Octopus bimaculoides DHPR alpha1 and RyR genes were retrieved from the Metazome v. 3.2 database from the University of California, and conserved protein domains were assessed using the NCBI Conserved Domain Database. DHPR alpha1 and RyR protein sequences were aligned with the human sequences using ClustalW and similarities were calculated using BLASTP at NCBI GenBank.

(e) Immunohistochemistry

Live dissociated muscle cells (see protocol above) were incubated in blocking solution (ASW-1% BSA) for 1 h and then suspended with 1 nM tetramethylrhodamine-α-bungarotoxin (Sigma) in blocking solution for 1 h. After the incubation, cells were washed 6 times × 5 min with ASW, centrifuged for 10 min at 500 RPM and re-suspended in ASW. The cells were then imaged with confocal microscopy (Fluoview 1000, Olympus, Tokyo, Japan).

AChR localization in arm tissue was visualized as follows. Transverse sections of arms approximately 100 µm thick were cut with a vibratome and incubated with 5 nM α-bungarotoxin ATTO-633 (Alomone labs) in blocking solution (PBS + 0.1% Triton X-100 (PBS-T) + 10% goat serum) for 2 h in the dark. Tissues were rinsed several times with PBS-T, post-fixed with 4% ASW and mounted with ProLong Gold antifade reagent (Life Technologies, Milan, Italy) for investigation.

To visualize the position of the AChR relative to the cell axis, a double staining was performed by incubating 100 µm frozen arm sections for 2 h in the dark with: Alexa Fluor 488 α-bungarotoxin (Thermo Fisher Scientific) diluted 1 : 700 in blocking solution + Alexa Fluor™ 647 Phalloidin (F-actin; Life Technologies, Milan, Italy) diluted 1 : 200 in blocking solution. Nuclei were then counterstained, incubating sections for 2 h at RT with Hoechst (nuclei; 1 : 1000).

DHPR and RYR labellings were performed on arm slices; 20 µm frozen sections were rinsed in 1× PBS, permeabilized in PBS-T two times × 5 min at RT and incubated in blocking solution (PBS-T + 10% goat serum) for 1 h at RT. Mouse DHPR alpha1 (1 : 200, Thermo Fisher Scientific) and rabbit RyR3 (1 : 1000, Millipore) primary antibodies were diluted in blocking solution and applied overnight at 4°C. After several PBS-T washes, sections were incubated respectively in Alexa-488 anti-mouse and Alexa-568 anti-rabbit secondary antibodies (1 : 1000 in blocking solution) and Hoechst (nuclei; 1 : 1000) for 2 h at RT. Tissues were rinsed several times and mounted in ProLong Gold antifade reagent (Life Technologies, Milan, Italy) for analysis.

Arm slices were imaged using an inverted confocal laser microscope (SP8, Leica Microsystems GmbH, Wetzlar, Germany), and three-dimensional reconstructions were generated using Leica Application Suite X software (LAS-X). Measurements of AChR dimensions were performed using ImageJ.

(f) Statistical analysis

Statistical analyses were performed using SigmaPlot 13.0 (Systat Software, Inc.). Normality of the dataset was first assessed with a normality test (Shapiro Wilk). *t*-Test and Kruskal–Wallis One Way Analysis of Variance on Ranks were used to assess discrepancy among experimental groups. p-Value < 0.05 were considered significant ($^*p < 0.05$, $^{***}p < 0.001$). Data in histograms are reported as means ± s.e.m.

3. Results and discussion

(a) Functional organization of the AChR at the NMJ

The octopus arm is composed almost entirely of spindle-shaped muscle cells tapering sharply to a point; cell lengths are non-normally distributed with a peak at approximately 700–900 µm (electronic supplementary material, figure S1). The localization and distribution of ACh receptors (AChR) were first characterized by labelling the nicotinic AChR in arm samples and in isolated muscle fibres. In both the longitudinal (L) muscles and trabeculae of the transverse muscle (T), AChR were oriented along the main muscle cell axis in an area surrounding the centre of the cells (figure 2—cf. confocal 3D projections in *a* (0°), *b* (90°*x*), *c* (90°*y*); figure 2*d*). This result was confirmed in isolated muscle fibres; AChR were concentrated in a single eye-shaped area at the centre of the cell where they overlapped with membrane invaginations, likely reflecting a postsynaptic junction structure (figure 2*e*). There was no significant difference in the length of the receptor sites between L and T, its mean length being approximately 16 µm (figure 2*f*; $n = 37$ in longitudinal and $n = 31$ in transverse muscles; *t*-test, $p = 0.42$). That is, the receptors site showed a similar arrangement irrespective of the muscle group.

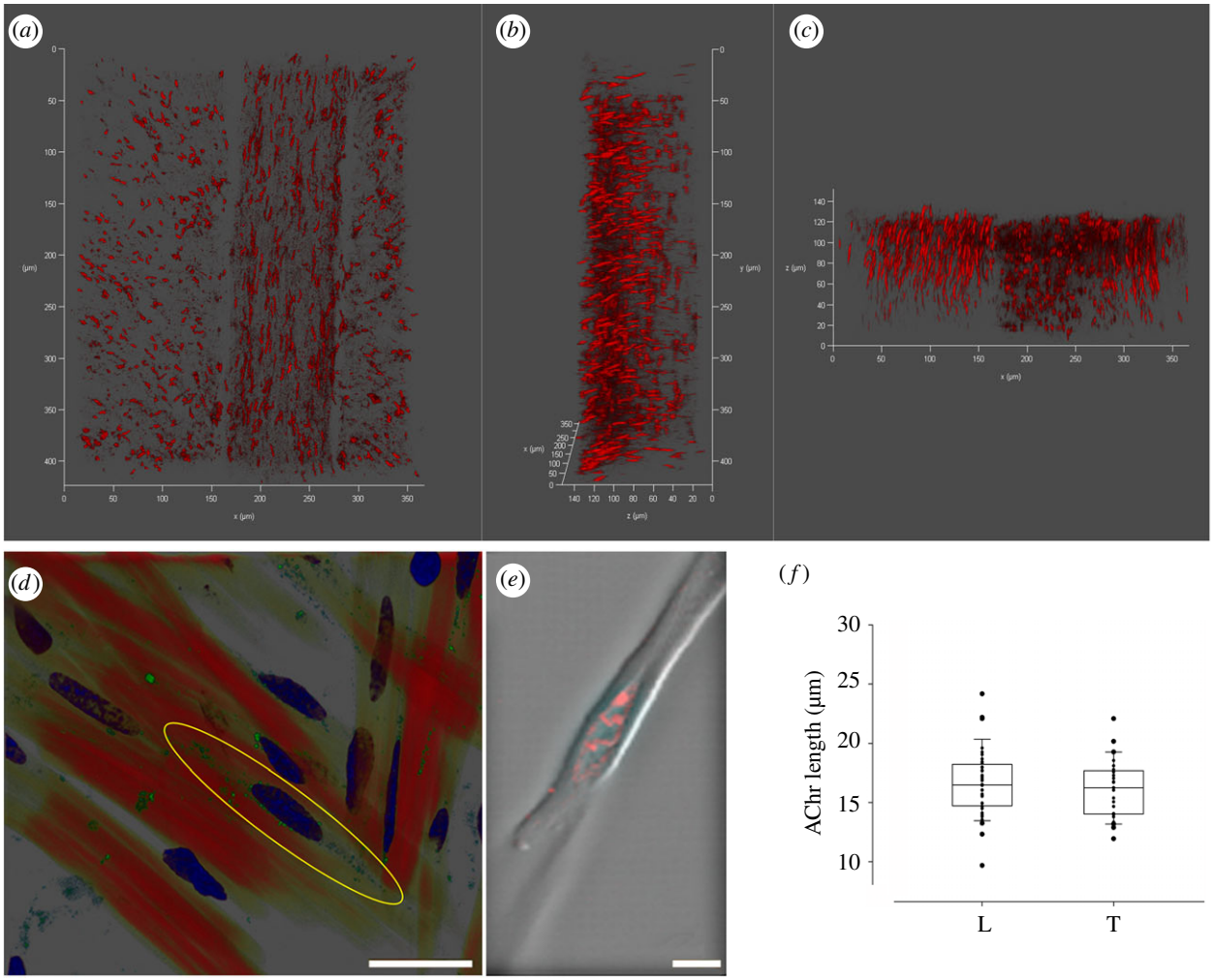

Figure 2. Localization of AChR in the octopus arm muscle. (*a*,*b*,*c*) Confocal 3D projections of an arm transverse section at 0°, 90°*x* and 90°*y*, respectively. Both L and T (trabeculae) muscles are visible and show the same longitudinal arrangement of the AChR (fluorescently labelled with α-bungarotoxin ATTO-633). (*d*) Confocal image of arm transverse section (T muscles) showing single muscle cells in red (F-actin labelled with phalloidin), AChR in green (fluorescently labelled with Alexa Fluor 488 α-bungarotoxin) and nuclei in blue (DAPI). The localization of the AChR in a central area around the nucleus is highlighted by a yellow ellipse. (*e*) Tetramethylrhodamine-α-bungarotoxin labelling of AChR in an isolated muscle cell as seen under a confocal microscope. AChR are concentrated in an eye-shaped structure at a single site forming hill-like structures in a central area around the nucleus. (*f*) Length of the AChR in longitudinal (L) and transverse (T) muscles show no significant differences (*t*-test, $p = 0.42$). Scale bars: (*d*) 25 µm; (*e*) 5 µm.

The presence of AChR was functionally assessed through the application of 1 mM ACh puffed by air pressure through a micropipette close to isolated muscle cells during whole-cell patch-clamp recording. This treatment evoked membrane depolarization that, if strong enough, could trigger typical fast action potentials (figure 3*a*). The micropipette was moved and ACh was puffed at different locations along the cell. This revealed characteristic depolarizing responses increasing in amplitude in a distance-dependent manner towards the centre of the cell (figure 3*b*,*c*, $n = 10$), while the response delay, quantitatively depicted in figure 3*c*, decreased towards the cell centre. Hence, the magnitude of the depolarization and speed of response are negatively correlated with the distance of the ACh application from the cell centre. This spatial and temporal response pattern fits the immunohistochemistry evidence of AChR localization at the cell centre (figure 2*d*,*e*).

(b) The electrophysiological properties of the NMJ

The AChR ionic current properties were characterized by voltage clamping. As shown in figure 4*a*,*b* the current/voltage relationship (IV curve) revealed a linear relationship between the amplitude of ACh-dependent current and membrane potential, with a reversal potential at around −10 mV. This suggests a close to equal contribution of Na^+ and K^+ currents, similar to the vertebrate NMJ [23]. To confirm this, we applied ACh in close proximity to the cell centre under three different conditions: Na^+ free ($n = 6$), low Na^+ (approx. 10% of the normal ASW ($n = 5$)) and normal ASW ((normal Na^+, 460 mM) ($n = 34$)). As depicted in figure 4*c*,*d* the ACh-dependent variation of membrane potential showed a statistically significant difference among the three conditions (Kruskal–Wallis one-way analysis of variance on ranks, $^{**}p < 0.001$).

We then tested the desensitization characteristic of the octopus AChR. The ACh-dependent response did not decline during at least 2 s of ACh application (figure 5*a*) or following repetitive ACh applications (figure 5*b*; $n = 19$), indicating that in contrast to other NMJ [24,25] this AChR lacks significant desensitization.

(c) Characterization of muscle excitation–contraction coupling

The octopus muscle action potential (AP) is primarily mediated by a calcium current through L-type voltage-gated

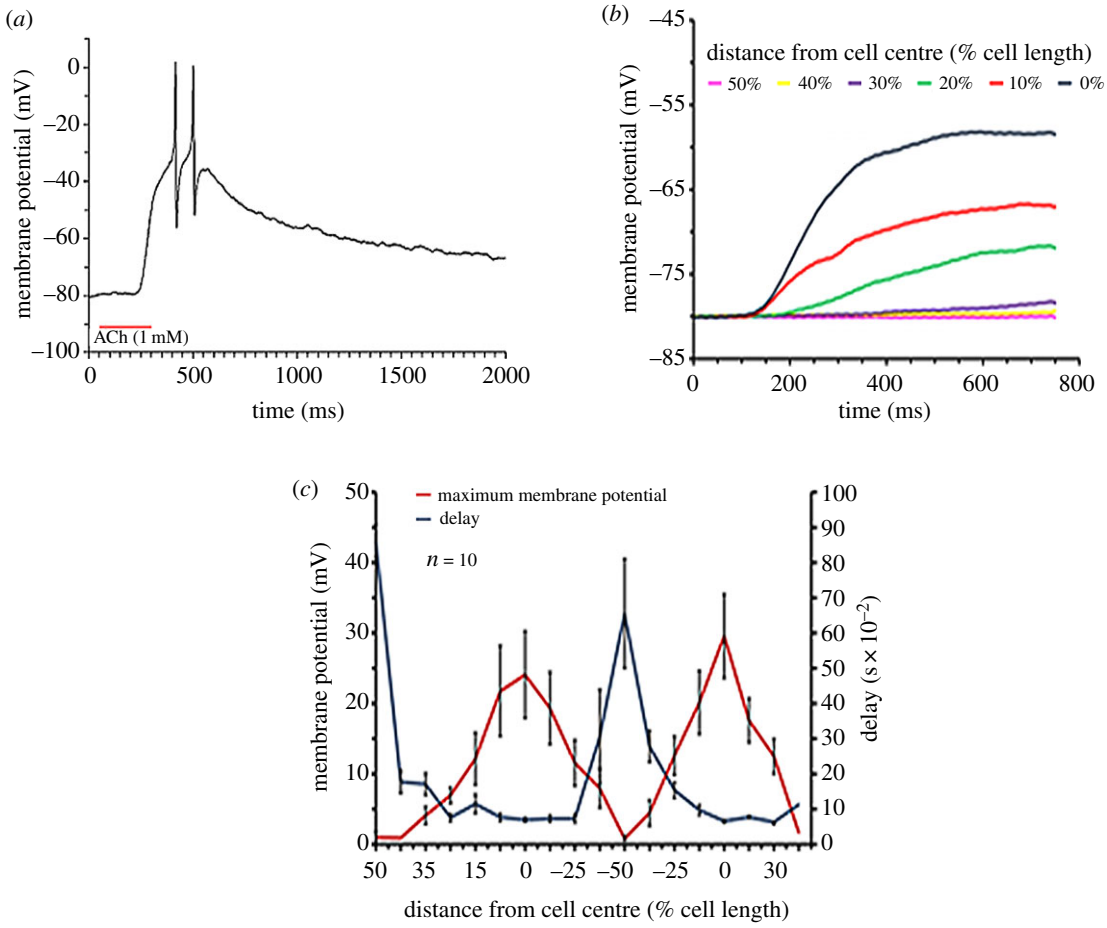

Figure 3. Physiological characterization of the central localization of AChR in octopus muscle cells. (*a*) Application of a few nanolitres of ACh (1 mM) close to the cell caused depolarization that could reach the APs threshold. (*b*) Typical recordings showing the membrane potential response to ACh injection at different distances along the cell. The distance with respect to the cell's centre is shown in % of total cell length. (*c*) Membrane potential response and the delays from ACh application as a function of the relative distance (% of cell length) of ACh injection site from the centre of the muscle cell. Each experiment was performed on a single cell. In each experiment, the ACh injecting pipette was moved from one end of the cell (indicated by 50%) to the other (indicated by −50%) and back. The results are reported as average ± s.e.m. ($n = 10$). (Online version in colour.)

channels [22]. Because the muscle cells are electrically compact, the AP is likely not required for propagating the electrical signals along the muscle cell as is the case in vertebrate muscle cells. That the AP of the octopus muscle cells is mediated by Ca^{2+}, rather than Na^{+}, suggests that these APs play a direct role in activating the contractile machinery.

To further investigate this point, muscle cells were stimulated by current injection in Ca^{2+} free ASW ($n = 16$), and membrane potential and contraction response were monitored. Figure 6*a* shows that replacing the normal ASW with Ca^{2+} free ASW eliminated the AP, and muscle contractions could no longer be induced. A similar response was obtained from applying ACh close to the cell centre in the same Ca^{2+} free condition (electronic supplementary material, figure S2). External Ca^{2+} is thus necessary for both the generation of the AP and contraction.

A transient increase in cytosolic Ca^{2+} concentration may also be mediated by Ca^{2+} release from internal Ca^{2+} stores. The octopus muscle cells lack the typical sarcoplasmic reticulum but present similar submembrane structures, defined as subsarcolemmal cisternae (or terminal cisternae), that may function as intracellular Ca^{2+} stores [1]. We, therefore, tested the possibility that internal Ca^{2+} stores are involved in muscle contraction [26–28]. Muscle cells were suspended in Ca^{2+}-free ASW and 10 mM of caffeine was applied with no additional stimulation. This caused a slow transient membrane depolarization accompanied by cell contraction (figure 6*b*). As the Ca^{2+}-free external ASW also contained EGTA, the contraction was likely due to caffeine-induced Ca^{2+} release from internal stores [27,28]. Membrane depolarization could be explained by calcium removal from the cytosol by the electrogenic Na^{+}/Ca^{2+} exchanger or through Ca^{2+} activated nonselective cation current [29–33]. However, the exact mechanism of this depolarization in octopus muscle cells requires further investigation, since the role of Ca^{2+}-dependent membrane currents varies among animals and in different tissues [34]. This set of experiments suggests that both internal and external sources of calcium ions can contribute to muscle contraction and that the release of Ca^{2+} from intracellular stores (such as the terminal cisternae) is induced by an inrush of external Ca^{2+} rather than by voltage as in vertebrate skeletal muscles [35].

To reveal the relative roles of external and internal Ca^{2+} in the development of cell contraction we perfused muscle cells with normal ASW and stimulated them through the patch pipette by raising the injected current in steps every 20 s until an action potential and cell contraction were observed (figure 7; electronic supplementary material, movie S3). The lowest stimulus inducing contraction was

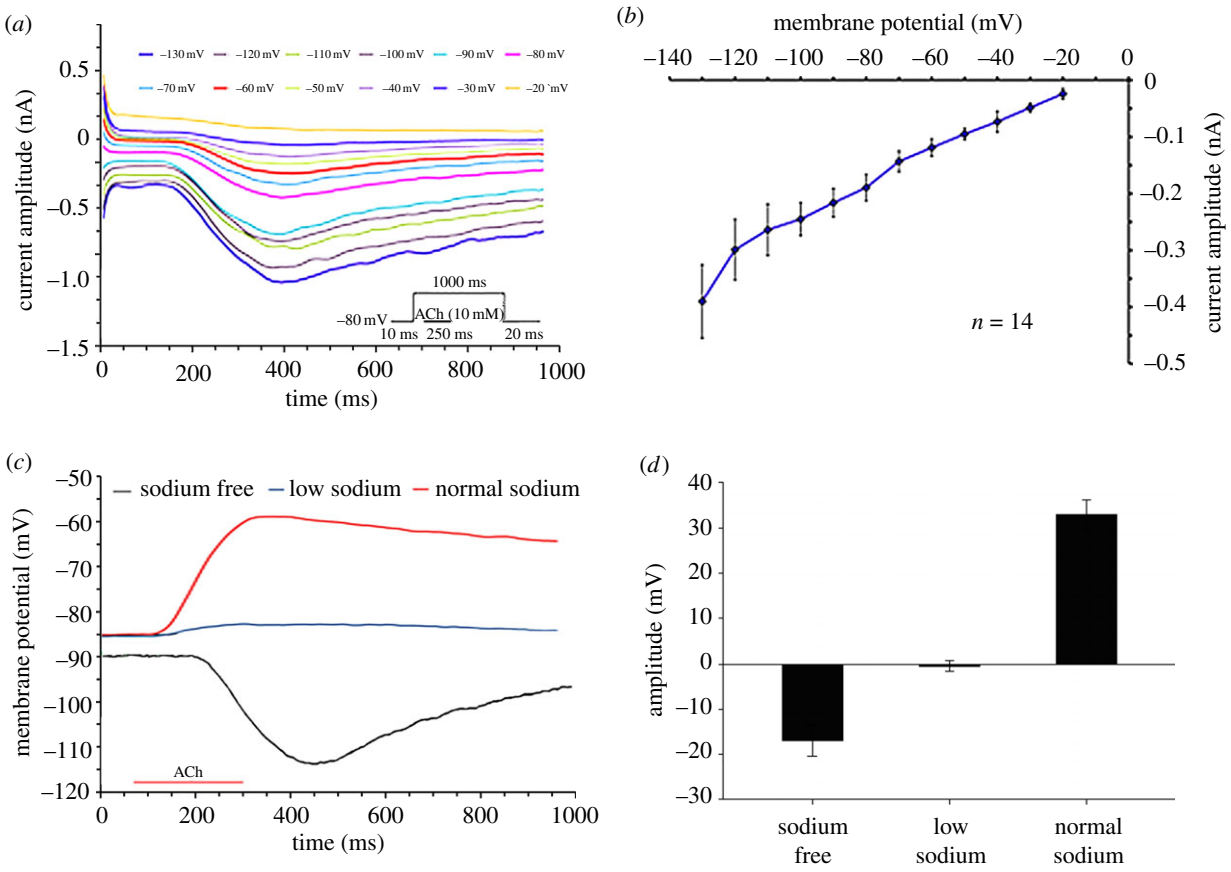

Figure 4. Electrophysiological characterization of the ACh-induced membrane current. (*a*) Example of voltage-clamp experiment showing the current time course and amplitude as a function of 12 voltage step commands. Each voltage step is indicated by a different colour. (*b*) Voltage–current curve of the ACh-induced current (average ± s.e.m., $n = 14$). The current was elicited by injection of 1 mM ACh for 250 ms during 1000 ms voltage steps of 10 mV from a holding potential of −80 mV. The relationships are close to linear with extrapolated reversal potential value close to −10 mV. (*c*) Current-clamp experiments showing the time course of the voltage response to the application of ACh under three conditions: normal Na^+ (red line), low Na^+ concentration buffer (blue line), Na^+-free ASW (black line). Note the minor ACh-induced depolarization in reduced Na^+ concentration and the hyperpolarizing ACh-response in Na^+ free solution. (*d*) Average ± s.e.m. of the ACh-induced maximal changes in membrane potential in the three ionic conditions is shown in (*c*) (Na^+ free, $n = 6$; Low Na^+, $n = 5$; Normal Na^+, $n = 34$ cells). (Online version in colour.)

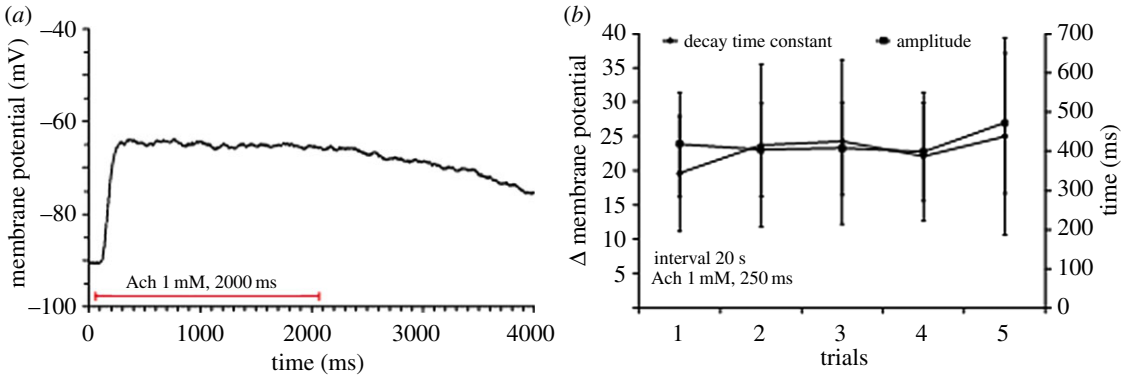

Figure 5. The response of isolated arm muscle cells to ACh did not desensitize. (*a*) A typical recording showing that the ACh-induced depolarization remained stable throughout a long period of ACh application, indicating no or a marginal AChR desensitization. (*b*) Depolarization induced by repetitive ACh injections (250 ms duration at 20 s intervals). Neither the response amplitudes nor the post ACh injection decay time-constant changed significantly over time ($n = 4$). The decay time constant was determined by fitting the results to the exponential equation: $V(t) = V_{(amp)}\ (e^{-t/C})$, ($V_{(amp)}$ = voltage at the end of ACh injection, t = time following injection, C = time constant). (Online version in colour.)

defined as the 'control' stimulation value (figure 7*a*). We then applied 10 mM of caffeine through the perfusion system to induce depletion of the Ca^{2+} from internal stores. After the initial caffeine-dependent depolarization and contraction (as in figure 6*b*) cells relaxed and the stimulation procedure was then repeated in the presence of caffeine. Here, although APs were evoked, no contraction was observed (figure 7*b*,*c*) until stimulation values (current amplitude × stimulus duration) reached approximately 400% (401.4 ± 55.86% ($n = 3$)) of the control stimulation (figure 7*d*). Thus, during caffeine-

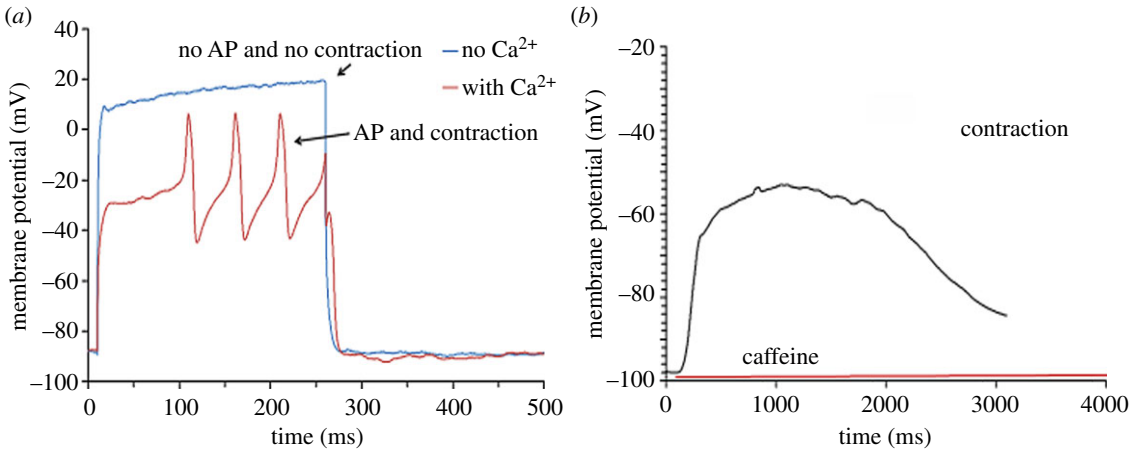

Figure 6. The role of Ca^{2+} in octopus muscle cell contraction. (*a*) Isolated muscle cells in ASW responded to current injection with an APs and contraction. Neither AP nor contractions were observed in response to current injection after replacement of normal ASW with Ca^{2+}-free ASW. (*b*) Application of 10 mM of caffeine evoked membrane depolarization and muscle cell contraction in cells suspended in Ca^{2+}-free EGTA ASW. (Online version in colour.)

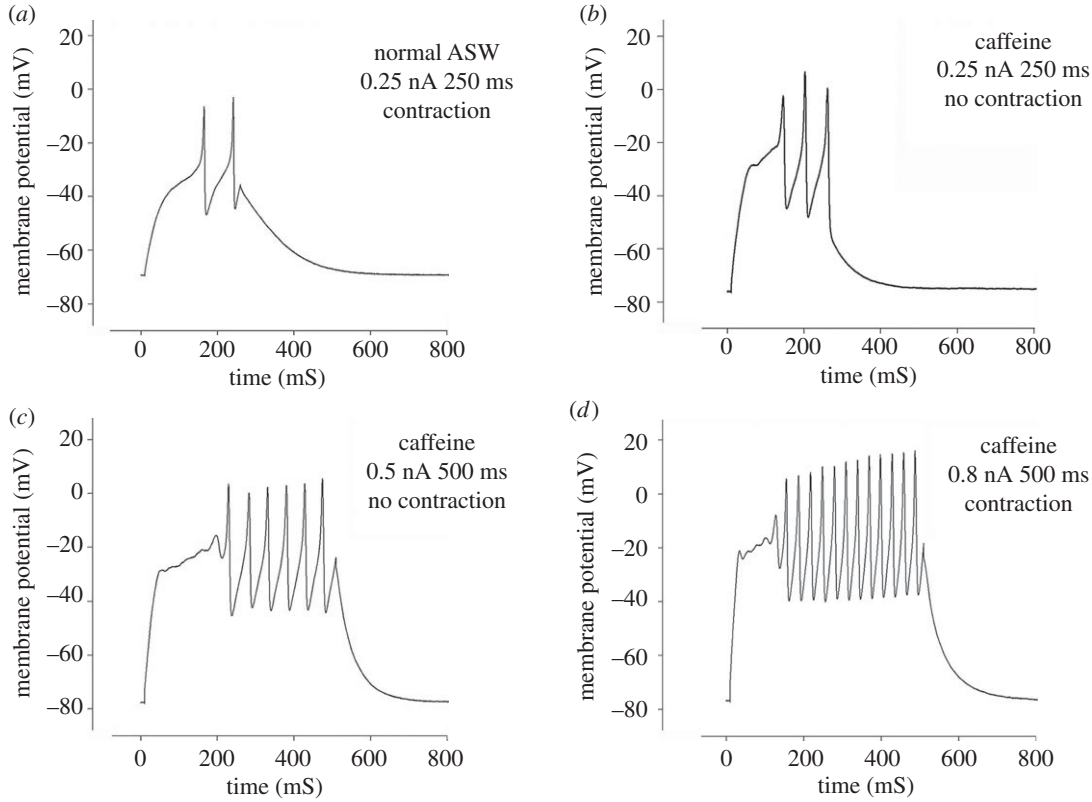

Figure 7. The effect of caffeine on muscle cell contraction. (*a*) A muscle cell in normal ASW responded to 0.25 nA stimulation with APs and contraction. (*b*,*c*) Following caffeine-induced depletion of internal Ca^{2+} stores (indicated by cell relaxation and membrane repolarization). (*b*) The cell responded with APs but no contraction was observed even at strong stimulation higher than in control (compare *a* with *b*,*c*). (*d*) Contraction responses were obtained in the presence of caffeine only after strong stimulation (approximately 400% of that in (*a*)).

induced depletion of the internal store, the action potential was still able to evoke contraction but this happened only at a higher threshold.

The difference in E-C characteristics revealed with caffeine (figure 7) suggests that Ca^{2+}-dependent Ca^{2+} release (CICR) from intracellular stores contributes to cell contraction. This mechanism is likely to be driven by Ca^{2+} entering via voltage-dependent Ca^{2+} channels as depolarization in Ca^{2+}-free external solution did not trigger contraction and depolarization alone is insufficient for activating calcium release from intracellular stores (figure 6*a*). Thus, calcium release from intracellular stores appears to be voltage-independent and to play a fundamental role in muscle contraction. Yet, the finding that contraction can be induced after depletion of the internal Ca^{2+} stores suggests that Ca^{2+} entering through Ca^{2+} channels may also contribute directly to muscle contraction, especially during vigorous activation of the muscle cells. These results suggest that octopus muscle cells possess a unique E-C mechanism that governs cell contraction both directly through external Ca^{2+} current during the action potential and indirectly through a CICR mechanism.

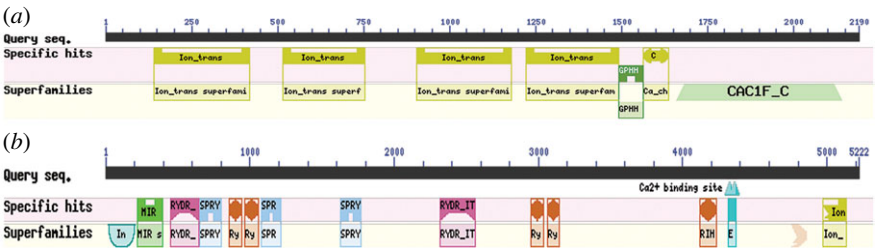

Figure 8. *Octopus bimaculoides* DHPR alpha1 subunit (*a*) and RyR (*b*) conserved domains. (*a*) Note the conservation of the four homologous repeats of transmembrane helices (Ion_trans) that constitute the pore and the voltage-gated calcium channel IQ domain (Ca_chan_IQ,) regulating cellular calcium flux. (*b*) In the RyR sequence, we could identify three SPRY domains, important for protein–protein interaction that may represent docking sites for DHPR, EF-hands and Ca^{2+} binding sites at the C terminal domain. (Online version in colour.)

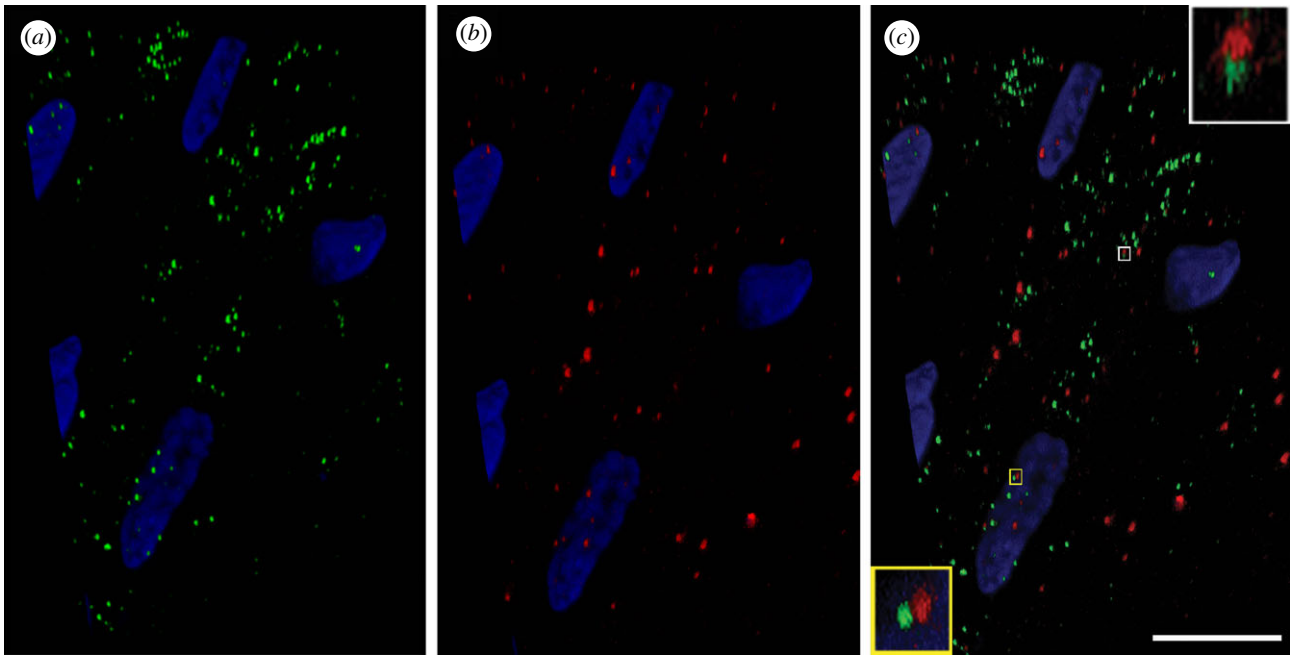

Figure 9. Immunofluorescence localization of DHPR alpha1 (*a*) and RyR3 (*b*) on a section of longitudinal arm muscle fibres (Alexa-488 anti-mouse and Alexa-568 anti-rabbit secondary antibodies respectively). These proteins are distributed along muscle cells and localized in close proximity at specific points (*c*), (see also *insets in c*); (DHPR: green; RyR3: red; nucleus: blue (DAPI)). Scale bar (*c*): 10 µm.

(d) Identification of RYRs and DHPRs in the muscle support CICR mechanism

The canonical mechanism involved in CICR from internal stores requires the existence and function of proteins such as the DHPR–RyR complex on the sarcoplasmic reticulum [36]. To test for the CICR mechanism in the octopus muscle cells we used genomic informatics and immunohistochemistry labelling to identify the presence and arrangement of proteins such as the DHPR–RyR complex on the subsarcolemmal cisternae (the octopus analogous of the sarcoplasmic reticulum). We searched particularly for dihydropyridine receptors (DHPR), which belongs to the high-voltage-activated family of voltage-gated calcium channels like the L-type Ca^{2+} channel that probably mediates the Ca^{2+} current identified in octopus muscle cells [22]. We also investigated the presence of ryanodine receptor families (RyRs) that mediates Ca^{2+} release from internal stores. These channels play a major role in the E-C coupling of striated and cardiac muscles [37].

The bioinformatics analysis identified the predicted DHPR alpha1 subunit and RyR in the sequenced genome of the closely related *Octopus bimaculoides* [38]. We found that octopus DHPR alpha1 subunit (2190 amino acidic residues) shares 62% of amino acids identity and has a 75% similarity with the human alpha1 subunits of the L-type voltage-dependent calcium channel. The main sites involved in the channel functions are well conserved (figure 8*a*). They include four homologous repeats of transmembrane helices (Ion_trans) that constitute the pore, the voltage-gated calcium channel IQ domain (Ca_chan_IQ) that regulates cellular calcium flux and a GPHH motif closely associated with IQ and found in voltage-dependent L-type calcium channel proteins in eukaryotes. Octopus RyR shared 50% identity of amino acids with the human voltage-independent RyR type3, which control the resting calcium ion concentration in skeletal muscles. Main domains involved in the channel functions are conserved; among these, three SPRY domains, important for protein–protein interaction and representing docking sites for DHPR, EF-hands, and Ca^{2+} binding sites at the C terminal domain [39] have been identified (figure 8*b*).

DHPR and RyR were detected on octopus muscle fibres using human monoclonal and polyclonal antibodies, respectively; both receptors were found to be scattered along the cells (figure 9*a*,*b*). The confocal images in figure 9*c* show a detailed co-distribution analysis and 3D reconstruction of

the double-labelled samples, where the two proteins are frequently visible in close proximity at specific locations across the sarcolemma (figure 9*c*, insets). These locations may correspond to the presence of subsarcolemmal cisternae.

DHPR and RyR are known to be important for linking cell membrane events to intracellular compartments such as the sarcoplasmic reticulum. Consequently, the rise of cytoplasmic calcium induced by extracellular Ca^{2+} influx through L-type calcium channels (DHPR receptors) will activate the RyRs that mediate Ca^{2+} release from internal stores (in the octopus, the subsarcolemmal or terminal cisternae) [35,40]. It is, therefore, reasonable to assume that this topological organization represents the functional link between sarcolemmal events and the voltage-independent release of calcium from intracellular stores. We identified RyR type3. These receptors are voltage-independent and are possibly activated through a CICR process [36]. This further supports the suggestion that the rise in cytosolic calcium is responsible for muscle contraction mediated by a voltage-independent CICR process.

(e) A comparative overview: the octopus neuromuscular system is unique

We have shown that the octopus muscle cells respond to ACh in a restricted area lying around the centre of the cell close to the cell nucleus and where AChR are concentrated. This region has an eye-shaped hill-like structure and was heavily stained for AChR in dissociated muscle cells and arm musculature preparations (figure 2). All muscle cells, irrespective of which muscle group they belong to (longitudinal or transverse), showed a similar pattern of AChR clustering. This fits with previous findings that the muscle cells in the different orientation groups are comprised of similar morphological and physiological units [2,7]. This feature is likely to simplify motor control because it implies that the relationship between motoneuronal activity and muscle mechanical output is constant in all muscle groups and, therefore, the anatomical organization of the muscles in the arm is an important factor in constraining the arm motor output.

The neuromuscular system of molluscs is highly diversified. For example in molluscs, excitatory nerves can activate brief phasic responses or prolonged tonic contractions, responsible for the passive catch state, depending on the specific properties of muscles and their innervating neurons. Individual muscle fibres may be innervated by a single or poly excitatory neurons (which can be either cholinergic or glutamatergic) or by dual, inhibitory and excitatory neurons [41]. This variability in molluscs neuromuscular configuration is probably due to the functional diversity of the different muscular systems and therefore our findings here likely represent an evolutionary adaptation of a molluscan neuromuscular system to achieve an efficient motor control of long and flexible hydrostatic arms (see [21]).

To better understand the functional implications of our findings, it is useful to compare the organization of the octopus arm NMJ with those typical of striated muscles in appendages of both vertebrates and invertebrates (electronic supplementary material, figure S4).

The octopus arm NMJ maintains the polyneuronal pattern of innervation typical for invertebrates, but the NMJ of each of the motoneurons with the postsynaptic AChR occur at a single postsynaptic site (endplate) as in vertebrate skeletal muscles (uniterminal innervation). This is an unusual innervation pattern for invertebrates, especially compared to arthropods, where the motoneuron axon terminals form many synaptic junctions (multiterminal innervation) along the entire length of muscle cells (electronic supplementary material, figure S4). These differences can, at least partly, be attributed to the very large and long dimension of the arthropods muscle cells relative to the small and electrotonically compact muscle cells of the octopus arm [2,7].

This phylogenetic comparative anatomical assessment of the octopus arm neuromuscular system agrees strikingly with the dimensions and the excitable properties of striated muscle cells in vertebrate and arthropods. In vertebrate skeletal muscles, the EPSPs at the localized NMJ (endplate) evoke a fast Na^{+} action potential that propagates along the long muscle fibre, activating the voltage-dependent contractile machinery. The arthropod muscle cells are usually unexcitable and contraction is regulated through a uniform depolarization of the entire cell induced by the multiterminal innervation along the cell. In sharp contrast, the octopus muscle cells are small and electrically compact [7], meaning that EPSPs at the centre of the cell control the membrane potential of the entire cell, eliminating the need for multispatial innervation or for action potentials propagation along the muscle cell (electronic supplementary material, figure S4). It is, therefore, conceivable that the voltage-gated Ca^{2+} channels can mediate both subthreshold Ca^{2+} entry along the entire cell and action potential-driven massive entry of extracellular calcium, activating vigorous contraction. This spiking activity, which is rare in molluscan muscle cells, is similar to that recorded in the special molluscan catch muscles [42].

4. Conclusion

Based on the E-C properties of octopus arm muscle cells, it is tempting to speculate that these cells rely on two different activation modalities. In the first mode, a low stimulus intensity generates a small Ca^{2+} influx through the voltage-gated Ca^{2+} channels, which activates CICR from the internal stores and may induce a graded range of contractions. The second mode is activated by stronger stimuli causing a robust Ca^{2+} influx to the cytosol through the voltage-gated Ca^{2+} channels. This, in addition to the induction of a robust Ca^{2+} release from internal stores, can also directly activate the contractile machinery leading to a vigorous contraction. Moreover, this current may maintain a high cytosolic Ca^{2+} level that leads to a stronger and longer contraction, even after the total release of Ca^{2+} from the internal stores and the $[Ca^{2+}]_i$-dependent inactivation process of the RYRs, as reported in other systems [37,43]. The electrical compactness of the muscle cells ensures that all these events effectively activate the contraction mechanism over the entire cell.

That muscle activation involves several activation modes conforms well to the unique polyneuronal innervation previously reported [7,44] and the properties of the NMJ and AChR revealed here. Each muscle cell is innervated by three distinct cholinergic inputs, each with a distinct postsynaptic response [7,44], indicating that each motoneuron may be engaged in mediating different modes of activation. The large synaptic inputs may activate what we described above as the vigorous activation mode, reaching the high

threshold for activation of Ca^{2+} spikes, while those with lower amplitudes may regulate the graded contraction through frequency-dependent summation of EPSP trains. These AChR lack desensitization properties, differing from the nicotinic AChR in vertebrates NMJ [25,45]. This suggests that this non-desensitizing property is especially suitable for a continuous membrane depolarization by a barrage of EPSPs bombarding a single junctional postsynaptic site. This may be important, for example, for the motoneurons with small EPSPs in tonically controlling steady muscle tension. Desensitization of the postsynaptic receptors would impair such a tonic modulation. In this scenario, the motoneurons with exceptionally large EPSPs are perfect for bringing the membrane potential into high voltage ranges, leading to a vigorous contraction mode that would trigger phasic actions and strong contraction or stiffening of muscles. It is very likely that this polyneuronal innervation of the muscular system is implemented for example, in the independent neuronal control of muscle stiffness (tonic control) and the contraction/actuation dynamics (phasic control).

Our results, therefore, suggest that in the octopus the different motoneuronal pools innervating each muscle cell in the arm are likely involved in activation of different E-C coupling modes, thus enabling the control system to recruit the appropriate dynamics of muscles activation. Possibly this mode of control has evolved for allowing efficient switching between functioning as a dynamical skeletal element, formed by stiffening, or as an actuator for motion generation.

Ethics. Experiments performed in Italy were approved by the Institutional Review Board and by the Italian Ministry of Health (authorization n. 465/2017-PR). Experiments performed in Israel were not subject to national legislation but our research conformed to the ethical principles of the three Rs (replacement, reduction and refinement) and of minimizing of animal suffering, following the Directive 2010/63/EU (Italian D. Lgs. n. 26/2014) and the guidelines in Fiorito *et al*. [46,47].

Data accessibility. All data are available as electronic supplementary material, data files S1 and S2.

Authors' contributions. N.N., L.Z. and B.H. developed the ideas and drafted the manuscript. N.N., T.S. and F.M. performed the experiments. L.Z. and N.N. analysed the data and performed the statistical analyses. All authors contributed to the manuscript and gave final approval for publication.

Competing interests. The authors declare no competing interests.

Funding. This work was supported by the EU COST ACTION FA1301 and by STIFF-FLOP IP: EU 7th Framework Program (FP7-ICT-2011.7), project no. 287728.

Acknowledgements. We thank local anglers from the Italian and Israeli Mediterranean coast for animal collection from the wild and Riccardo Navone of the animal facility for animal care and maintenance. For the generous contribution of tetramethylrhodamine-α-bungarotoxin at the preliminary stages of the project we thank professor Lily Anglester and Eran Finkel from the Department of Medical Neurobiology, Hebrew University-Hadassah Medical School, Jerusalem, Israel.

References

1. Kier WM, Smith KK. 1985 Tongues, tentacles and trunks: the biomechanics of movement in muscular-hydrostats. *Zool. J. Linn. Soc.* **83**, 307–324. (doi:10.1111/j.1096-3642.1985.tb01178.x)
2. Feinstein N, Nesher N, Hochner B. 2011 Functional morphology of the neuromuscular system of the Octopus vulgaris arm. *Vie Milieu* **61**, 219–229.
3. Kier WM. 2016 The musculature of coleoid cephalopod arms and tentacles. *Front. Cell Dev. Biol.* **4**, 10.
4. Hanassy S, Botvinnik A, Flash T, Hochner B. 2015 Stereotypical reaching movements of the octopus involve both bend propagation and arm elongation. *Bioinspir. Biomim.* **10**, 035001. (doi:10.1088/1748-3190/10/3/035001)
5. Yekutieli Y, Sagiv-Zohar R, Aharonov R, Engel Y, Hochner B, Flash T. 2005 Dynamic model of the octopus arm. I. Biomechanics of the octopus reaching movement. *J. Neurophysiol.* **94**, 1443–1458. (doi:10.1152/jn.00684.2004)
6. Yekutieli Y, Sagiv-Zohar R, Hochner B, Flash T. 2005 Dynamic model of the octopus arm. II. Control of reaching movements. *J. Neurophysiol.* **94**, 1459–1468. (doi:10.1152/jn.00685.2004)
7. Matzner H, Gutfreund Y, Hochner B. 2000 Neuromuscular system of the flexible arm of the octopus: physiological characterization. *J. Neurophysiol.* **83**, 1315–1328. (doi:10.1152/jn.2000.83.3.1315)
8. Flash T, Hochner B. 2005 Motor primitives in vertebrates and invertebrates. *Curr. Opin. Neurobiol.* **15**, 660–666. (doi:10.1016/j.conb.2005.10.011)
9. Sumbre G, Fiorito G, Flash T, Hochner B. 2006 Octopuses use a human-like strategy to control precise point-to-point arm movements. *Curr. Biol.* **16**, 767–772. (doi:10.1016/j.cub.2006.02.069)
10. Sumbre G, Gutfreund Y, Fiorito G, Flash T, Hochner B. 2001 Control of octopus arm extension by a peripheral motor program. *Science* **293**, 1845–1848. (doi:10.1126/science.1060976)
11. Richter JN, Hochner B, Kuba MJ. 2015 Octopus arm movements under constrained conditions: adaptation, modification and plasticity of motor primitives. *J. Exp. Biol.* **218**, 1069–1076. (doi:10.1242/jeb.115915)
12. Richter JN, Hochner B, Kuba MJ. 2016 Pull or push? Octopuses solve a puzzle problem. *PLoS ONE* **11**, e0152048. (doi:10.1371/journal.pone.0152048)
13. Gutnick T, Byrne RA, Hochner B, Kuba M. 2011 Octopus vulgaris uses visual information to determine the location of its arm. *Curr. Biol.* **21**, 460–462. (doi:10.1016/j.cub.2011.01.052)
14. Zullo L, Sumbre G, Agnisola C, Flash T, Hochner B. 2009 Nonsomatotopic organization of the higher motor centers in octopus. *Curr. Biol.* **19**, 1632–1636. (doi:10.1016/j.cub.2009.07.067)
15. Hochner B. 2012 An embodied view of octopus neurobiology. *Curr. Biol.* **22**, R887–R892. (doi:10.1016/j.cub.2012.09.001)
16. Hochner B. 2008 Octopuses. *Curr. Biol.* **18**, R897–R898. (doi:10.1016/j.cub.2008.07.057)
17. Zullo L, Fossati SM, Imperadore P, Nodl MT. 2017 Molecular determinants of cephalopod muscles and their implication in muscle regeneration. *Front. Cell Dev. Biol.* **5**, 53. (doi:10.3389/fcell.2017.00053)
18. Fossati SM, Benfenati F, Zullo L. 2011 Morphological characterization of the *Octopus vulgaris* arm. *Vie Milieu* **61**, 197–201.
19. Zullo L, Fossati SM, Benfenati F. 2011 Transmission of sensory responses in the peripheral nervous system of the arm of *Octopus vulgaris*. *Vie Milieu* **61**, 197–201.
20. Hochner B. 2013 How nervous systems evolve in relation to their embodiment: what we can learn from octopuses and other molluscs. *Brain Behav. Evol.* **82**, 19–30. (doi:10.1159/000353419)
21. Levy G NN, Zullo L, Hochner B. 2017 Motor control in soft-bodied animals. In *The Oxford handbook of invertebrate neurobiology* (ed. JH Byrne). New York, NY: Oxford University Press.
22. Rokni D, Hochner B. 2002 Ionic currents underlying fast action potentials in the obliquely striated muscle cells of the octopus arm. *J. Neurophysiol.* **88**, 3386–3397. (doi:10.1152/jn.00383.2002)
23. Takeuchi A, Takeuchi N. 1960 On the permeability of end-plate membrane during the action of transmitter. *J. Physiol.* **154**, 52–67. (doi:10.1113/jphysiol.1960.sp006564)
24. McGehee DS, Role LW. 1995 Physiological diversity of nicotinic acetylcholine receptors expressed by vertebrate neurons. *Annu. Rev. Physiol.* **57**, 521–546. (doi:10.1146/annurev.ph.57.030195.002513)

25. Giniatullin R, Nistri A, Yakel JL. 2005 Desensitization of nicotinic ACh receptors: shaping cholinergic signaling. *Trends Neurosci.* **28**, 371–378. (doi:10.1016/j.tins.2005.04.009)
26. Bhat MB, Zhao J, Zang W, Balke CW, Takeshima H, Wier WG *et al.* 1997 Caffeine-induced release of intracellular Ca^{2+} from Chinese hamster ovary cells expressing skeletal muscle ryanodine receptor: effects on full-length and carboxyl-terminal portion of Ca^{2+} release channels. *J. Gen. Physiol.* **110**, 749–762. (doi:10.1085/jgp.110.6.749)
27. Dani JA, Eisenman G. 1984 Acetylcholine-activated channel current–voltage relations in symmetrical Na^+ solutions. *Biophys. J.* **45**, 10–12. (doi:10.1016/S0006-3495(84)84087-4)
28. Shirokova N, Garcia J, Rios E. 1998 Local calcium release in mammalian skeletal muscle. *J. Physiol.* **512**, 377–384. (doi:10.1111/j.1469-7793.1998.377be.x)
29. Callewaert G, Cleemann L, Morad M. 1989 Caffeine-induced Ca^{2+} release activates Ca^{2+} extrusion via Na^+-Ca^{2+} exchanger in cardiac myocytes. *Am. J. Physiol.* **257**, C147–C152. (doi:10.1152/ajpcell.1989.257.1.C147)
30. Solaro R, Moss R. 2002 *Molecular control mechanisms in striated muscle contraction*. Dordrecht, The Netherlands: Springer Netherlands.
31. Varro A, Negretti N, Hester SB, Eisner DA. 1993 An estimate of the calcium content of the sarcoplasmic reticulum in rat ventricular myocytes. *Pflugers Arch.* **423**, 158–160. (doi:10.1007/BF00374975)
32. Danaceau JP, Lucero MT. 2000 Electrogenic Na^+/Ca^{2+} exchange. A novel amplification step in squid olfactory transduction. *J. Gen. Physiol.* **115**, 759–768. (doi:10.1085/jgp.115.6.759)
33. Schlotthauer K, Bers DM. 2000 Sarcoplasmic reticulum Ca^{2+} release causes myocyte depolarization: underlying mechanism and threshold for triggered action potentials. *Circ. Res.* **87**, 774–780. (doi:10.1161/01.RES.87.9.774)
34. Koster OF, Szigeti GP, Beuckelmann DJ. 1999 Characterization of a $[Ca^{2+}]_i$-dependent current in human atrial and ventricular cardiomyocytes in the absence of Na^+ and K^+. *Cardiovasc. Res.* **41**, 175–187. (doi:10.1016/S0008-6363(98)00202-8)
35. Tanabe T, Beam KG, Adams BA, Niidome T, Numa S. 1990 Regions of the skeletal muscle dihydropyridine receptor critical for excitation-contraction coupling. *Nature* **346**, 567–569. (doi:10.1038/346567a0)
36. Niggli E, Lederer WJ. 1990 Voltage-independent calcium release in heart muscle. *Science* **250**, 565–568. (doi:10.1126/science.2173135)
37. Laver DR. 2018 Regulation of the RyR channel gating by Ca^{2+} and Mg^{2+}. *Biophys. Rev.* **10**, 1087–1095. (doi:10.1007/s12551-018-0433-4)
38. Albertin CB *et al.* 2015 The octopus genome and the evolution of cephalopod neural and morphological novelties. *Nature* **524**, 220–224. (doi:10.1038/nature14668)
39. Tae H, Casarotto MG, Dulhunty AF. 2009 Ubiquitous SPRY domains and their role in the skeletal type ryanodine receptor. *Eur. Biophys. J.* **39**, 51–59. (doi:10.1007/s00249-009-0455-8)
40. Rebbeck RT, Karunasekara Y, Board PG, Beard NA, Casarotto MG, Dulhunty AF. 2014 Skeletal muscle excitation-contraction coupling: who are the dancing partners? *Int. J. Biochem. Cell Biol.* **48**, 28–38. (doi:10.1016/j.biocel.2013.12.001)
41. Muneoka Y, Twarog BM. 1993 Neuromuscular transmission and excitation–contraction coupling in molluscan muscle. In *The Mollusca* (eds ASM Saleuddin, KM Wilbur), pp. 35–76. New York, NY: Academic Press.
42. Heyer CBK SB, Karlsson UL. 1973 Neuromuscular systems in molluscs. *Am. Zool.* **13**, 247–270. (doi:10.1093/icb/13.2.247)
43. Cully TR, Edwards JN, Launikonis BS. 2014 Activation and propagation of Ca^{2+} release from inside the sarcoplasmic reticulum network of mammalian skeletal muscle. *J. Physiol.* **592**, 3727–3746. (doi:10.1113/jphysiol.2014.274274)
44. Gutfreund Y, Matzner H, Flash T, Hochner B. 2006 Patterns of motor activity in the isolated nerve cord of the octopus arm. *Biol. Bull.* **211**, 212–222. (doi:10.2307/4134544)
45. Auerbach A, Akk G. 1998 Desensitization of mouse nicotinic acetylcholine receptor channels: a two-gate mechanism. *J. Gen. Physiol.* **112**, 181–197. (doi:10.1085/jgp.112.2.181)
46. Fiorito G *et al.* 2014 Cephalopods in neuroscience: regulations, research and the 3Rs. *Invert. Neurosci.* **14**, 13–36. (doi:10.1007/s10158-013-0165-x)
47. Fiorito G *et al.* 2015 Guidelines for the care and welfare of cephalopods in research—a consensus based on an initiative by CephRes, FELASA and the Boyd Group. *Lab. Anim.* **49**(2 Suppl), 1–90. (doi:10.1177/0023677215580006)